RSC Advances

ROYAL SOCIETY OF CHEMISTRY

www.rsc.org/advances

Journal Name

ARTICLE

A unified approach toward the rational design of selective low nanomolar human neutrophil elastase inhibitors

Received 00th January 20xx,
Accepted 00th January 20xx

DOI: 10.1039/x0xx00000x

www.rsc.org/

L. R. P. Areias,[a,†] E. F. P. Ruivo,[a,†] L. M. Gonçalves,[a] M. T. Duarte,[b] V. André,[b] R. Moreira,[a] S. D. Lucas [a,*] and R. C. Guedes[a,*]

A computer-aided campaign boosted the discovery of potent human neutrophil elastase (HNE) inhibitors. A pharmacophoric model was developed, validated and applied to filter an oxo-beta-lactam library previously generated by *de novo* design. This campaign led us to compound **1** which showed an inhibitory activity of 6.9 nM against HNE, more active than the only commercially available HNE inhibitor for therapeutic usage. Computer-aided methodologies proved again to be powerful tools to increase the rate of success for HNE inhibitor discovery either for therapeutic or activity-based probing development.

Introduction

Unregulated elastolytic activity caused by an imbalance between human neutrophil elastase (HNE) and its endogenous inhibitors is on the basis of several life-threatening diseases such as chronic obstructive pulmonary disease (COPD), currently the third leading cause of death worldwide, cystic fibrosis, acute respiratory distress syndrome and acute lung injury.[1] More recently, evidence was also found on HNE-related processes involvement in non-small cell lung cancer progression.[2] Therefore, HNE is an attractive therapeutic target for lung diseases but besides the efforts at academic and industrial level, no HNE inhibitor launched the market successfully. The exception is Sivelestat (ONO-5046) from Ono Pharmaceuticals that is administrated in Japan in acute lung conditions, nevertheless failed FDA approval. Although a large number of low molecular-weight HNE inhibitors, covering a wide range of chemical scaffolds with different mechanisms of action were reported over the last decades, there is still an urgent need to optimize drug discovery process toward HNE therapeutic target.[1] Moreover, being HNE a potential biomarker for lung diseases it is extremely important to develop new scaffolds as specific substrates for HNE activity-based probe (ABP) development. Recently, the application of HNE specific ABPs revealed that the amount of active HNE during the process of neutrophil extracellular trap formation was not so high as expected, revealing the utility of this approach in dissecting biological events.[3]

Computer-aided methodologies are valuable tools toward time and resource sparing on a drug discovery process. Although virtual screening methodologies previously allowed us to identify valuable hits with new chemical scaffolds for HNE inhibition,[4, 5] the efficiency of this methodology is often low due to a wide range of possible dynamic conformations adopted by the enzyme active-site[6, 7] and for the specific case of HNE it is an induced-fit binding mode that most likely rules its activity.[8, 9] To overcome this problem we developed and optimized a unified approach to boost HNE inhibitor discovery and generated a 3D pharmacophoric model toward HNE activity that reflects tridimensional features for potent HNE inhibitors, leading to a powerful tool for compound making decision.[10] An oxo-beta-lactam template was further used for automated *de novo* design as it was discovered by our group as a potent HNE inhibitor.[11, 12] The validated pharmacophore was used to filter a virtual library generated by *de novo* design and promising hits were synthesized for proof-of-concept. Using this approach we were able to obtain low nanomolar inhibitors and validate a methodology for the generation of innovative chemical motifs for HNE drug discovery.

Results and discussion

To the best of our knowledge two pharmacophoric models have been developed for HNE. Greene *et al.*[13] built a pharmacophoric model based on the interactions of the crystallographic complex between HNE and methoxysuccinyl-Ala-Ala-Pro-alanine inhibitor, nevertheless no hit activities were reported for validation purpose. Habash *et al.*[14] recently

[a] *Research Institute for Medicines (iMed.ULisboa), Faculty of Pharmacy, Universidade de Lisboa. Av. Professor Gama Pinto, 1649-003 Lisbon, Portugal. E-mail: sdlucas@ff.ulisboa.pt; rguedes@ff.ulisboa.pt*
[b] *Centro de Química Estrutural, Instituto Superior Técnico, Universidade de Lisboa,1049-001 Lisboa, Portugal.*
† These authors contributed equally.
Electronic Supplementary Information (ESI) available: computational methods description, molecular data sets for pharmacophoric generation and validation, docking poses for compound **1**, chemical synthesis, NMR spectra, X-ray crystallographic data for compounds **1** and **3** and detailed description on biochemical assays. See DOI: 10.1039/x0xx00000x

also reported a pharmacophoric model based on a known inhibitor training set leading to hit identification with discreet μM activities. In the present work we generate a ligand-based pharmacophoric model with MOE (Molecular Operating Environment) software.[15] Different pharmacophore queries were built either by using pharmacophore elucidator or flexible alignment and pharmacophoric consensus available in MOE package, varying also the annotation schemes and different training set combinations from a group of 20 potent HNE inhibitors (full data available at supporting info). In MOE, 3D pharmacophoric models contain locations of the common features or chemical groups as well as restrictions on shape. The distance and angles between features may be refined by validation against positive and negative controls (test set). To optimize our pharmacophore we set a positive control with 106 structurally diverse HNE inhibitors with activities bellow 5 μM and a negative control with 99 molecules that when tested against HNE showed no inhibitory activity (Test set, n=205, data available at supporting info). Several pharmacophoric models were generated in order to evaluate the potential to discriminate between actives and inactives when assayed against the test set (Figure 1).

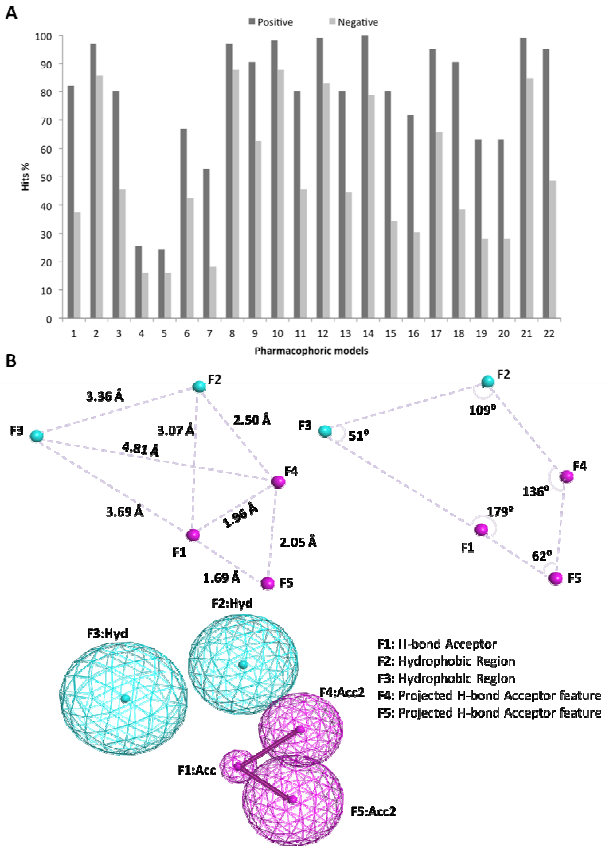

Figure 1. A) Hit percentage for different ligand-based farmacophore hypothesis. B) Detailed scheme for optimized features, distances and angles for optimal discrimination between actives and inactives from the test set, starting from phamacophoric model 18. Performed with MOE2012.10 software.

The most discriminative model (pharmacophoric hypothesis 18, Figure 1) was further optimized concerning feature size and distances between features to obtain the final pharmacophoric model (Figure 1) that includes two hydrophobic features (F2 and F3), one hydrogen bond acceptor (F1) and two projected hydrogen bond acceptors (F4 and F5). This optimized model successfully identifies 92% of the molecules of the positive control as hits, while it only detects 35% of false positives from the negative control. Therefore, this data validate this model as a suitable tool to filter molecular databases, as the generated phamacophoric model efficiently represents the chemical features necessary for HNE inhibition, assisting compound making decisions.

Oxo-β-lactams were discovered in our group as potent HNE inhibitors. A diethyl substitution pattern was found to be optimal for S1 subsite recognition, nevertheless the most active compound was found to be active, although in lower extent, against parent serine proteases and susceptible to plasma enzymatic activity. Thus, to overcome this problem, we decided to use the oxo-β-lactam scaffold with a diethy substitution as a template to generate new compounds using automated *de novo* design in order to improve substitution pattern on the amine counterpart (Figure 2), as there is an urgent need for HNE inhibitors as efficient drugs toward a variety of lung diseases. The new library based on the oxo-β-lactam scaffold was assembled using *Add Group to Ligand* tool implemented in MOE2012.10 software package which includes a fragment database obtained from drug-like molecules. The algorithm generated 2370 potential small HNE inhibitors with molecular weight below 510 $gmol^{-1}$. This virtual library was then filtered using the obtained pharmacophoric model and the generated hits were docked into the HNE active site to infer about preferred location and interactions with HNE active site, using GOLD 5.1 software.[16] Due to the induced-fit character of HNE inhibition, molecular docking was performed using different HNE crystallographic structures including the free enzyme (PDB-ID: 3Q76), the HNE-dihydropyrimidone complex (PDB-ID: 3Q77) and the HNE-chlorometylketone complex (PDB-ID: 1HNE), so that we could infer on possible recognition counterparts. After docking calculations analysis, compound **1** (Figure 2) was found as the most promising molecule and was selected for chemical synthesis. Docking poses of compound **1** showed important π-π stacking with Phe192 either when docked on the free enzyme with a narrower active-site but also in the complexed structures, pointing up the possibility to block the access to the active site serine by strong recognition in the S1 subsite, (docking poses available on supporting information). Moreover, the hydrazine moiety was envisaged to improve hydrolytic stability.

Synthesis of the selected oxo-β-lactam **1** was performed by a cyclisation reaction of the corresponding hydrazine building block with diethylmalonyl dichloride using reported methodologies and its structural assignment was performed by X-ray crystallography (data available at supporting information).[12, 17] As predicted, when assayed against HNE compound **1** showed to be a potent HNE inhibitor with an IC_{50} value of 6.9 nM (Table 1), a break-through result as it has a

lower IC_{50} than the commercial Sivelestat (IC_{50} = 14.7 nM in our assay).

Suitable ligand-efficiency value (LE = 0.39) and high lipophilic ligand-efficiency (LLE = 4.88) point out that oxo-β-lactam **1** may be an exceptional lead for drug development. Motivated by this exceptional result we decided to synthesize a simpler analogue, **2**, to check for LE improvement and also bioisosteres **3** and **4**. In fact, we found that the absence of a second aromatic counterpart decreased HNE activity (Table 1), suggesting that extra-recognition on the S1 or S2/S1'subsites is determinant for potency. Sulfonyl hydrazine analogue **3** showed no inhibitory activity toward HNE and we believe that this is due to its slightly acidic character (calculated pK_a = 5.2), leading to a deprotonated species under physiological pH, as the methylated analogue **4** showed to inhibit HNE with an IC_{50} value of 108.2 nM. Hence, inhibitory character was lost by reducing the recognition elements of the lead **1**, nevertheless the LE was slightly increased for compounds **2** and **4** with values of 0.46 and 0.43, respectively.

During last years, HNE inhibitors have been abandoned in several stages of clinical trials for a variety of reasons, most likely related to low selectivity for parent proteases. We evaluate the selectivity of the synthesized compounds toward a careful selection of serine proteases (Table 1) and very fortunately we observed that lead compound **1** was selective toward, at least, eight closely related serine proteases (SI >1000). This result might be explained by the specificity conferred by the benzylamine counterpart toward HNE as the acyl-hydrazine **2** presents a weaker selectivity toward PPE, Thrombin and Chymotrypsin (SI = 27, 7 and 4, respectively).

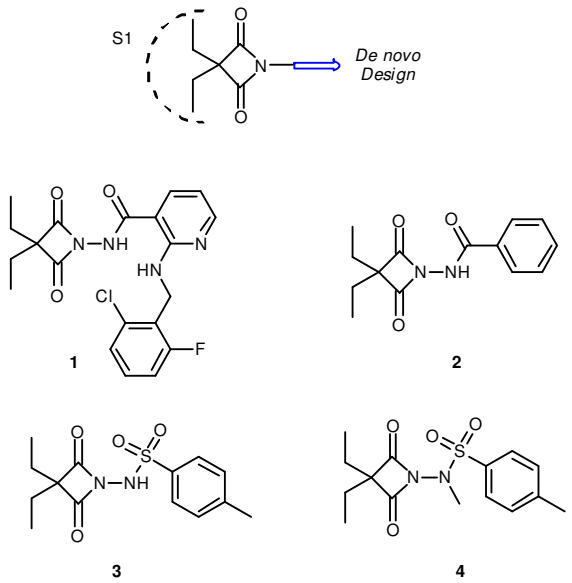

Figure 2. *De novo* design of oxo-β-lactam-based HNE inhibitors (some examples selected for synthesis).

Table 1. Activity toward HNE and selectivity.

Compd	IC_{50} (nM)	IC_{50} (μM)							
	HNE	PPE	Pr3	CatG	Urokinase	Kallikrein	Thrombin	Trypsin	Chymotrypsin
1	6.9±0.06	8.6±1.3	>50	>50	>50	>50	>50	>50	>50
2	367±19	22.7±1.2	>50	>50	>50	>50	6.1±1.1	>50	3.5±1.1
3	>5000	nd[a]	nd[a]	nd[a]	nd[a]	nd[a]	nd[a]	nd[a]	nd[a]
4	108.2±6	25.2±1.1	>50	>50	>50	>50	>50	>50	>50
ONO-5046	14.7±0.6	>50	>50	>50	>50	>50	>50	>50	>50

[a] nd-non determined

Table 2. Stability and cytotoxicity assays.

	$t_{1/2}$		
	pH 7.4 Buffer	Human Plasma	Rat microssomes
1	11.1±0.1h	26.5±2.5m	3.9±0.5m
ONO-5046	stable[a]	stable[a]	19.9±0.7m

[a] stable after 48h.

On the other hand, the sulfonylhydrazine **3** showed to be selective toward the proteases tested (SI > 500 except for PPE). Hence, the selectivity of oxo-β-lactams **1** and **3** is an outstanding result to be explored for further development of these lead compounds for therapeutic and ABP application. These results prove the benefit of using *in silico* combined methodologies and allow us to discover an incredibly potent HNE inhibitor. Moreover, compound **1** was also assayed for cytotoxicity and metabolic stability. Absence of toxicity was observed after exposure of mouse cell lines NIH3T3 and human cell lines HEK293T (IC_{50} > 100 μM), nevertheless low stability was observed with a discrete half-life of 26.5 min when incubated with human plasma and very low half-life of 3.9 min toward rat microssomes (Table 2), not adequate for oral administration but still tolerable for inhalatory administration with the aim of potential use as a lung-targeted drug.

Experimental

Pharmacophore Modelling

Ligand-based pharmacophore modelling was performed using MOE 2012.10 (Molecular Operating Environment) software.[15] Three sets of molecules were compiled for pharmacophore generation (training set, n=20, structural and activity data available at supporting info), a positive control (n=106, structurally diverse HNE inhibitors with activities bellow 5 μM for HNE – detailed data available at supporting info) and a negative control (n= 99, structurally diverse compounds that

when tested against HNE showed no inhibitory activity - detailed data at supporting info). The ligand-based pharmacophore query was built based on the flexible alignment of the training set. In MOE, 3D pharmacophoric models contain locations of the common features or chemical groups as well as restrictions on shape. Annotation points were generated using the PCHD system (Polar-charged-hydrophobic-directional) and the selected alignment options emphasized the aromatic atoms, donor atoms and acceptor atoms. For the best pharmacophoric models obtained at this stage the featurevolume radius as well as distance between features were refined by validation against positive and negative controls to afford the final pharmacophoric model presented herein (Figure 1).

De novo design

For the generation of a virtual library of oxo-β-lactams we performed *de novo* design using Add Group to Ligand tool from MOE.2012.10 package. As previously reported by our group diethyl substitution pattern was found to be optimal for HNE S1 subsite recognition of oxo-β-lactams and so we used the diethyl oxo-β-lactam scaffold for N-derivatization and defined this bond vector for fragment insertion. MOE package has an 800 000 drug-like fragment library and the generated molecules were filtered by molecular weight lower than 510 $gmol^{-1}$ leading to a library of 2370 potential HNE inhibitors.

Chemistry

2-((2-chloro-6-fluorobenzyl)amino)-N-(3,3-diethyl- azetidin-1-yl -2,4-dione)nicotinamide (1). To a solution of diethylmalonyl dichloride (1,88 mmol, 324 µl) in pyridine (3 ml) under nitrogen atmosphere was added dropwise a solution of 3-((2-chloro-6-fluorobenzyl)amino)isonicotinohydrazide (1,88 mmol, 768 mg) in pyridine (3 ml) and the reaction proceeded overnight at room temperature. Pyridine was co-evaporated with 3x toluene. The residue was purified by flash chromatography on silica gel using EtOAc/n-hexane gradient as eluent and after recrystalization from hexane the desired product was obtained as colorless crystals (16 mg, 2%) mp 156-158 °C; δ ^{1}H NMR (400 MHz, $CDCl_3$) 8.35-8.31 (m, 1H), 8.19 (s, 1H), 7.66 (d, J = 7.7 Hz, 1H), 7.23 (m, 2H), 7.05 – 6.99 (m, 1H), 6.53 (dd, J = 7.8, 4.8 Hz, 1H), 4.89 (d, J = 5.3 Hz, 2H), 1.88 (q, J = 15.2, 7.5 Hz, 4H), 1.10 (t, J = 7.1 Hz, 6H). ^{13}C NMR (101 MHz, $CDCl_3$) δ 204.4 (C2,4), 174.2 (C8), 165.5 (Pyr6), 157.4 (Ar2), 153.6 (Pyr4), 136.0 (Pyr2), 129.4 (Ar6), 125.4 (Ar1), 124.5 (Pyr4), 114.4 (Pyr2), 114.1 (Ar4), 110.9 (Ar5), 105.4 (Ar3), 66.9 (C3), 36.32 (C10), 23.4 (C5), 9.2 (C6). Calcd. ($C_{20}H_{20}ClFN_4O_3$): C, 57.35; H, 4.81; N, 13.38%. Found: C, 57.14; H, 4.81; N, 12.65%. **Crystal Data of compound 1.** $C_{20}H_{20}ClFN_4O_3$, M= 418.85, orthorhombic, a = 22.318(4), b = 10.108(3), c = 9.029(7) Å, V = 2036.9(17) Å^3, T = 298(2) K, space group $Pna2_1$ (Z = 4), 25820 reflections measured, 4092 unique (R_{int} = 0.0397) which were used in all calculations. The final $wR(F^2)$ was 1.059. Crystallographic Data for **1** as well as synthetic details for the synthesis of compounds **2**, **3** and **4** is given in supporting information.

Conclusions

Overall our results show the magnitude of computer-aided methodologies as powerful tools to increase the rate of successful HNE inhibitor discovery and disclosure a valuable pharmacophoric model as a potent tool to filter potential HNE inhibitor databases. A unified approach based on computer-aided techniques followed by an experimental proof-of-concept provided potent and selective oxo-β-lactams as promising lead compounds for a variety of lung diseases as well as a potential basis for ABP development.

Acknowledgements

The authors thank Dr. Maria Elisa Alves for providing human plasma samples collected from healthy volunteers, and the Fundação para a Ciência e a Tecnologia for financial support, Pest-OE/SAL/UI4013/2014, SFRH/BPD/64265/2009(SDL).

Notes and references

1. S. D. Lucas, E. Costa, R. C. Guedes and R. Moreira, *Medicinal Research Reviews*, 2013, **33**, E73-E101.
2. G. Moroy, A. J. P. Alix, J. Sapi, W. Hornebeck and E. Bourguet, *Anti-Cancer Agents in Medicinal Chemistry*, 2012, **12**, 565-579.
3. P. Kasperkiewicz, M. Poreba, S. J. Snipas, H. Parker, C. C. Winterbourn, G. S. Salvesen and M. Drag, *Proceedings of the National Academy of Sciences*, 2014, **111**, 2518-2523.
4. S. D. Lucas, L. M. Goncalves, T. A. F. Cardote, H. F. Correia, R. Moreira and R. C. Guedes, *MedChemComm*, 2012, **3**, 1299-1304.
5. F. Montalbano, P. M. S. D. Cal, M. A. B. R. Carvalho, L. M. Goncalves, S. D. Lucas, R. C. Guedes, L. F. Veiros, R. Moreira and P. M. P. Gois, *Organic & Biomolecular Chemistry*, 2013, **11**, 4465-4472.
6. G. Schneider, *Nature Reviews Drug Discovery*, 2010, **9**, 273-276.
7. Y. Tanrikulu, B. Kruger and E. Proschak, *Drug Discovery Today*, 2013, **18**, 358-364.
8. G. Hansen, H. Gielen-Haertwig, P. Reinemer, D. Schomburg, A. Harrenga and K. Niefind, *Journal of Molecular Biology*, 2011, **409**, 681-691.
9. S. G. Estacio, R. Moreira and R. C. Guedes, *Journal of Chemical Information and Modeling*, 2011, **51**, 1690-1702.
10. J. H. Van Drie, *Wiley Interdisciplinary Reviews: Computational Molecular Science*, 2013, **3**, 449-464.
11. J. Mulchande, R. C. Guedes, W. Y. Tsang, M. I. Page, R. Moreira and J. Iley, *Journal of Medicinal Chemistry*, 2008, **51**, 1783-1790.
12. J. Mulchande, R. Oliveira, M. Carrasco, L. Gouveia, R. C. Guedes, J. Iley and R. Moreira, *Journal of Medicinal Chemistry*, 2010, **53**, 241-253.
13. J. Greene, S. D. Kahn, H. Savoj, P. Sprague and S. L. Teig, *Journal of Chemical Information and Computer Sciences*, 1994, **34** , 1297-1308.
14. M. Habash, A. H. Abdelazeem and M. O. Taha, *Medicinal Chemistry Research*, 2014, **23**, 3876-3896.
15. MOE – Molecular Operating Environment MOE.2012 Chemical Computing Group: Montreal, www.chemcomp.com).
16. G. Jones, P. Willett and R. C. Glen, *Journal of Molecular Biology*, 1995, **245**, 43-53.
17. A. Ebnöther, E. Jucker, E. Rissi, J. Rutschmann, E. Schreier, R. Steiner, R. Süess and A. Vogel, *Helvetica Chimica Acta*, 1959, **42**, 918-955.